A TWO-DIMENSIONAL AND STEADY-STATE NUMERICAL MODEL OF THE PLANETARY BOUNDARY LAYER

Hu Yinqiao (胡隐樵), *Su Congxian* (苏从先), *Ge Zhengmo* (葛正谟)

Lanzhou Institute of Plateau Atmospheric Physics, Academia Sinica

Received June 5, 1986

ABSTRACT

In this paper, a two-dimensional and steady-state numerical model of the planetary boundary layer is developed. It includes the horizontal deformation of the eddy exchange coefficients and horizontal turbulence exchange. The difference between the structure of the heat island and cold island is analysed using this model.

I. FORMULATING THE PROBLEM

In the boundary layer we are concerned with meteorological phenomena generated on the local inhomogeneity of temperature. Examples include the breezes occurring at land/sea (lake) interfaces and the urban heat island generated by horizontal thermal differences between city and countryside. The "cold island effects" are generated also by horizontal thermal differences between a lake or an oasis and the desert. A two-level model, which is divided into the surface layer and the Ekman layer was commonly used for this kind of meteorological phenomena in the boundary layer for convenience sake. In the surface layer, the similarity theory which has been studied widely under horizontal homogeneous condition is commonly used in numerical model. But all the above meteorological phenomena happen due to the surface heterogeneity, so it is necessary to establish a numerical model of the planetary boundary layer for horizontal heterogeneity. For this reason, the horizontal heterogeneous shear of eddy coefficient in stream field and the horizontal turbulence exchange is considered in the control equation. Then the numerical model of the planetary boundary layer under horizontal heterogeneity is obtained.

II. THE BASIC EQUATIONS AND THE BOUNDARY CONDITIONS

The studied problem belongs to the meso-scale or small-scale. In considering the horizontal turbulence exchange, the two-dimensional and steady-state basic equations of the planetary boundary layer are given by

$$u\frac{\partial u}{\partial x}+w\frac{\partial u}{\partial z}=fv-\frac{1}{\rho}\frac{\partial P}{\partial x}+\frac{\partial}{\partial z}\left(k\frac{\partial u}{\partial z}\right)+\frac{\partial}{\partial x}\left(k_H\frac{\partial u}{\partial x}\right) \tag{1}$$

$$u\frac{\partial v}{\partial x}+w\frac{\partial v}{\partial z}=-f(u-U_g)+\frac{\partial}{\partial z}\left(k\frac{\partial v}{\partial z}\right)+\frac{\partial}{\partial x}\left(k_H\frac{\partial v}{\partial x}\right) \tag{2}$$

$$u\frac{\partial \theta}{\partial x}+w\frac{\partial \theta}{\partial z}=\frac{\partial}{\partial z}\left(k\frac{\partial \theta}{\partial z}\right)+\frac{\partial}{\partial x}\left(k_H\frac{\partial \theta}{\partial x}\right) \tag{3}$$

$$u\frac{\partial q}{\partial x}+w\frac{\partial q}{\partial z}=\frac{\partial}{\partial z}\left(k\frac{\partial q}{\partial z}\right)+\frac{\partial}{\partial x}\left(k_H\frac{\partial q}{\partial x}\right) \tag{4}$$

$$\frac{\partial u}{\partial x}+\frac{\partial}{\partial z}(\rho w)=0 \tag{5}$$

$$\frac{\partial}{\partial z}\left(\frac{P}{P_0}\right)^{\kappa}=-\frac{\kappa g}{R\theta} \tag{6}$$

$$P=\rho RT. \tag{7}$$

The equations and the symbols above are well known, but a horizontal diffusion term is added in Eqs. (1)-(4) considering the sudden changes in the thermodynamical state of the surface as in the cold island effect problem of the lake in the desert. The observation shows that the temperature on the lake is about 25°C, but that in the desert around the lake reaches 60°C. So the horizontal temperature difference of the air is very large under this strong temperature difference. It is about 1 °C/100 m near the bank. If the horizontal eddy coefficient k is the same as the perpendicular k, the horizontal diffusion term will be the same as the perpendicular, and therefore the horizontal diffusion term can not be omitted.

Now let us determine the eddy coefficient. According to turbulent theory, Heisenberg (1948) obtained the eddy coefficient under neutral stability:

$$k=\varepsilon^{1/3}l^{4/3}, \tag{8}$$

where l is the mixing length, ε is the turbulence energy dissipation per unit mass. It can be written as

$$\varepsilon=kS^2, \tag{9}$$

where S is a magnitude relating to the distortion of the stream field. From (8) and (9), the eddy coefficient of the stream field distortion under neutral stability can be written as

$$k=l^2S. \tag{10}$$

For non-neutral stability, Eq. (9) can be written as

$$k=l^2S\left[1-\frac{R_i}{R_{ic}}\right], \tag{11}$$

where R_i is the Richardson number, which can be written as

$$R_i=\frac{g}{\theta_s}\frac{\partial\bar{\theta}}{\partial z}/S^2. \tag{12}$$

For the two-dimensional problem, S is given by

$$S=\left[2\left(\frac{\partial u}{\partial x}\right)^2+2\left(\frac{\partial w}{\partial z}\right)^2+\left(\frac{\partial v}{\partial z}\right)^2+\left(\frac{\partial v}{\partial x}\right)^2+\left(\frac{\partial u}{\partial z}+\frac{\partial w}{\partial x}\right)^2\right]^{1/2}. \tag{13}$$

The mixing length l is represented in Blackadar (1962) form:

$$l=\frac{k_0(z-z_0)}{1+k(z+z_0)/\lambda}, \tag{14}$$

where k_0 is the Kaman constant. The result of Businger's (1971) observation shows that k_0 is equal to 0.35, which is used in calculation. The parameter z_0 is roughness and $\lambda=0.00027\,U_g/f$. There is no well-considered conclusion for the horizontal eddy coefficient, but according to Eq (8), $k\propto l^{4/3}$. From the original definition of the mixing length, the l in horizontal direction is larger than that in vertical direction. So we assume

$$k_H=\begin{cases}k & \text{for } R_i\geqslant R_{ic}\\ \alpha k & R_i<R_{ic},\end{cases} \tag{15}$$

α is a constant. Owing to the scarcity of the observation data, we assume α is equal to 3 in calculation. This does not influence the basic problem.

The upper and lower boundary conditions are:

$$u=v=w=0, \quad \text{for } z=0 \tag{16}$$

$$\theta=\theta(x,z=0), \quad q=q(x,z=0)$$

$$v=w=0, \quad u=U_g \quad \text{for } z=H \tag{17}$$

For the calculation stability the lateral boundary condition is:

$$\frac{\partial^2 u}{\partial x^2}=\frac{\partial^2 v}{\partial x^2}=\frac{\partial^2\theta}{\partial x^2}=\frac{\partial^2 q}{\partial x^2}=0 \quad \text{for } x=\pm L. \tag{18}$$

In our model $L=105$ km.

Eqs. (1)-(7) and (11) are closed for $u, v, w, \theta, q, p, \rho$ and k. The solutions can be obtained by using the boundary conditions.

In addition, the horizontal homogeneous field is used for the background field. It satisfies the following equations:

$$-f\bar{v}=-\frac{1}{\rho}\frac{\partial\bar{p}}{\partial x}+\frac{\partial}{\partial z}\left(\bar{k}\frac{\partial\bar{u}}{\partial z}\right) \tag{19}$$

$$f(\bar{u}-U_g)=\frac{\partial}{\partial z}\left(\bar{k}\frac{\partial\bar{v}}{\partial z}\right) \tag{20}$$

$$\frac{\partial}{\partial z}\left(\bar{k}\frac{\partial\bar{\theta}}{\partial z}\right)=C_1 \tag{21}$$

$$\frac{\partial}{\partial z}\left(\bar{k}\frac{\partial q}{\partial z}\right)=C_2 \tag{22}$$

$$\frac{\partial}{\partial z}\left(\frac{\bar{p}}{P_0}\right)^{\kappa}=-\frac{\kappa g}{R\bar{\theta}} \tag{23}$$

The eddy coefficient in the background field satisfies the interpolation relation (Pielke, 1974)

$$k=\begin{cases}k_0u_*z/\phi(z/L) & z<h\\ \bar{k}_H+\left(\dfrac{H-z}{H-h}\right)^2\left\{\bar{k}_h-\bar{k}_H-(z-h)\left[\left.\dfrac{\partial\bar{k}}{\partial z}\right|_{z=h}+\dfrac{2(\bar{k}_h-\bar{k}_H)}{H-h}\right]\right\}, & h\leqslant z\leqslant H\\ \bar{k}_H & z>H\end{cases} \tag{24}$$

where $\bar{k}_h$ and $\bar{k}_H$ are the eddy coefficients respectively at altitude h which is the depth of the surface layer, and at altitude H which is the depth of the planetary boundary. $\bar{k}_H=10^{-4}\text{m}^2/\text{sec}$. The function ϕ is decided from the stratification condition in the surface layer. The constants C_1 and C_2 are decided from the linked condition at altitudes h and H. For example, as $z=h$, $\bar{k}\frac{\partial\bar{\theta}}{\partial z}=-H_0/\rho\ C_p$, where H_0 is the sensible heat flux in the surface layer, as $z=H$, $\bar{k}_H=0$, thus constant C_1 is decided. Similarly, C_2 is decided.

III. THE SOLVING PROCESS

For convenience, Eqs .(1)-(4) are written in the form

$$g+\frac{1}{\rho}\frac{\partial P}{\partial x}-u\frac{\partial f}{\partial x}-w\frac{\partial f}{\partial z}+\frac{\partial}{\partial z}\left(k\frac{\partial f}{\partial z}\right)+\frac{\partial}{\partial x}\left(k_H\frac{\partial f}{\partial x}\right)=0, \tag{25}$$

where g is a term related to the geostrophic wind, f represents u, v, θ or q. The control Eqs. are solved by upstream difference. The grid points in both the x and z directions are represented by (i, k). For convenience, we define the symbols:

$$A_u=\begin{cases}\dfrac{u(i,k)}{x(i)-x(i-1)} & \text{for } u\geqslant 0\\[2ex] \dfrac{u(i,k)}{x(i+1)-x(i)} & u<0\end{cases} \tag{26}$$

$$A_w=\begin{cases}\dfrac{w(i,k)}{z(k)-z(k-1)} & \text{for } w\geqslant 0\\[2ex] \dfrac{w(i,k)}{z(k+1)-z(k)} & w<0\end{cases} \tag{27}$$

$$A_{k+1}=\frac{2k(i,k+1/2)}{[z(k+1)-z(k-1)][z(k+1)-z(k)]} \tag{28}$$

$$A_{k-1}=\frac{2k(i,k-1/2)}{[z(k+1)-z(k-1)][z(k)-z(k-1)]} \tag{29}$$

$$A_{kH+1}=\frac{2k_H(i+1/2,k)}{[x(i+1)-x(i-1)][x(i+1)-x(i)]} \tag{30}$$

$$A_{kH-1}=\frac{2k_H(i-1/2,k)}{[x(i+1)-x(i-1)][x(i)-(i-1)]} \tag{31}$$

$$A=A_u+A_w+A_{k+1}+A_{k-1}+A_{kH+1}+A_{kH-1}. \tag{32}$$

The difference of (25) is

$$R_f=-g(i,k)-R_p(i,k)+R_u(i,k)+R_w(i,k)+R_k(i,k)+R_{kH}(i,k) \tag{33}$$

where $g(i, k)$ is the term related to the geostrophic wind; the other terms are given in Table 1. R_f is the remainder of the difference computation. We will solve the equations for f as $R_f=0$. The difference equations corresponding to (5), (6) and (7) are obtained without difficulty.

Table 1

	$u\geqslant 0$	$u<0$
R_p	$\frac{1}{\rho}\frac{P(i,k)-P(i-1,k)}{x(i)-x(i-1)}$	$\frac{1}{\rho}\frac{P(i+1,k)-P(i,k)}{x(i+1)-x(i)}$
R_w	$(A_u+A_{kH-1})[f(i,k)-f(i-1,k)]$	$-(A_u-A_{kH+1})[f(i+1,k)-f(i,k)]$
R_{kH}	$-A_{kH+1}[f(i+1,k)-f(i,k)]$	$A_{kH-1}[f(i,k)-f(i-1,k)]$
	$w\geqslant 0$	$w<0$
R_w	$(A_w+A_{k-1})[f(i,k)-f(i,k-1)]$	$-(A_w-A_{k+1})[f(i,k+1)-f(i,k)]$
R_k	$-A_{k+1}[f(i,k+1)-f(i,k)]$	$A_{k-1}[f(i,k)-f(i,k-1)]$

To obtain the solution of a set of difference equations, the relaxation method is used to find their iterative formula. Assuming the remainders of the nth iteration to be $R_f^n(i,k)$, in the $(n+1)$th iteration, the $(n+1)$ th values are substituted into the iteration formula at the points $(i,k-1)$ and $(i-1,k)$ in the space which has been scanned, but at the points (i,k), $(i+1,k)$ and $(i,k+1)$ which have not been scanned, the nth values are used to be substituted into. Setting the $(n+1)$th iteration to reach the convergence condition, their remainders are all equal to zero. From equation (33) we obtain,

$$R_f^n(i,k) = -g^n(i,k) - R_p^n(i,k) + R_u^n(i,k) + R_v^n(i,k) + R_\theta^n(i,k) + R_{kH}^n(i,k). \tag{34}$$

The remainder of the $(n+1)$th iteration is

$$R_f^{n+1}(i,k) = 0 = -g^{n+1}(i,k) - R_p^{n+1}(i,k) + R_u^{n+1}(i,k) + R_v^{n+1}(i,k) + R_\theta^{n+1}(i,k) + R_{kH}^{n+1}(i,k) \tag{35}$$

Eq. (35) minus Eq. (34), after some operation, has the following iteration formulas:

$$f^{n+1}(i,k) = f^n(i,k) + \{F_u^n(i,k) + F_v^n(i,k) - R_f^n(i,k)\}/A^n \tag{36}$$

$$A^n = A_u^n + A_v^n + A_{k+1}^n + A_{k-1}^n + A_{kH+1}^n + A_{kH-1}^n \tag{37}$$

$$F_u^n = \begin{cases} (A_u^n - A_{kH+1}^n)[f^{n+1}(i-1,k) - f^n(i-1,k)] & u \geqslant 0 \\ (A_u^n + A_{kH-1}^n)[f^{n+1}(i+1,k) - f^n(i+1,k)] & u < 0 \end{cases} \tag{38}$$

$$F_v^n = \begin{cases} (A_v^n - A_{k+1}^n)[f^{n+1}(i,k-1) - f^n(i,k-1)] & w \geqslant 0 \\ (A_v^n + A_{k-1}^n)[f^{n+1}(i,k+1) - f^n(i,k+1)] & w < 0. \end{cases} \tag{39}$$

By using the above iteration formulas, $u^{n+1}(i,k)$, $v^{n+1}(i,k)$, $\theta^{n+1}(i,k)$ and $q^{n+1}(i,k)$ can be obtained. Then making use of the static equation, the equation of continuity and the equation of state, $P^{n+1}(i,k)$, $w^{n+1}(i,k)$ and $\rho^{n+1}(i,k)$ can be obtained without difficulty. From Eqs. (13) and (11), $S^{n+1}(i,k)$ can be calculated easily. In the iterative process, the boundary conditions, Eqs. (16)–(18), are used every time. The lateral conditions actually change into those at $x=-L$, $f^{n+1}(i,k) = 2f^{n+1}(i-1,k) - f^{n+1}(i-2,k)$, and at $x=+L$, $f^{n+1}(i,k) = 2f^{n+1}(i+1,k) - f^{n+1}(i+2,k)$. In the actual computation, the network grid puts $i=31$, $k=17$ and is divided nonuniformly. In the central region it is denser than in the side region.

To sum up, the iterative solving process is as follows:

1) The background field obtained from Eqs. (19)–(24) is used as the initial iterative field.

2) The corresponding remainder, and the iterative values of u, v, θ and q are got from Eqs. (34) and (36)–(39).

3) The iterative solutions of p, w, k and ρ are found.

4) Steps 2) and 3) are repeated up to the $(n+1)$ th iteration, until R_f^{n+1} satisfies the convergence condition, $R_f^{n+1} \leqslant \varepsilon$. Then the final iterants are the solutions which we need. In actual computation, we put $\varepsilon = 0.01$.

IV. COMPUTING EXAMPLES

1. *The Numerical Modeling of the Construction Characteristic of the Urban Heat Island*

It is well known that the temperature difference between the urban area and the countryside gives rise to the urban heat island. Research on the urban heat island and its influence on the diffusion process is of great significance for the urban microclimate and urban pollution, therefore the urban heat island is investigated extensively. Here a numerical experiment result

of the construction of the urban heat island is given. The parameters are obtained in the following way:

$f=8.57\times10^{-4}s^{-1}$; $P_0=850$ hPa; $u_*=0.4$ m/s; $U_g=10.0$ m/s; $h=100$ m; $H=1000$ m. The roughness of the underlying surface z_0 is

$$z_0=\begin{cases}0.5\text{ m} & \text{for } x_1\leqslant x\leqslant x_2 \text{ (in the urban heat island)}\\ 0.0002\text{ m} & x<x_1 \text{ or } x>x_2 \text{ (outside the urban heat island).}\end{cases} \tag{40}$$

In the computation, put $x_1=-5$ km, $x_2=5$ km. The lower boundary condition for $z=0$ is

$$u=v=w=0,$$
$$\theta=\begin{cases}\theta_0+\Delta\theta & x_1\leqslant x\leqslant x_2\\ \theta_0 & x<x_1,\ x>x_2\end{cases}$$
$$q=\begin{cases}q_0+\Delta q & x_1\leqslant x\leqslant x_2\\ q_0 & x<x_1,\ x>x_2,\end{cases} \tag{41}$$

and put $\theta_0=290^\circ$K; $\Delta\theta=5^\circ$C. Here q is the dust density, $q_0=900$ μg/m³; $\Delta q=11000$ μg/m³.

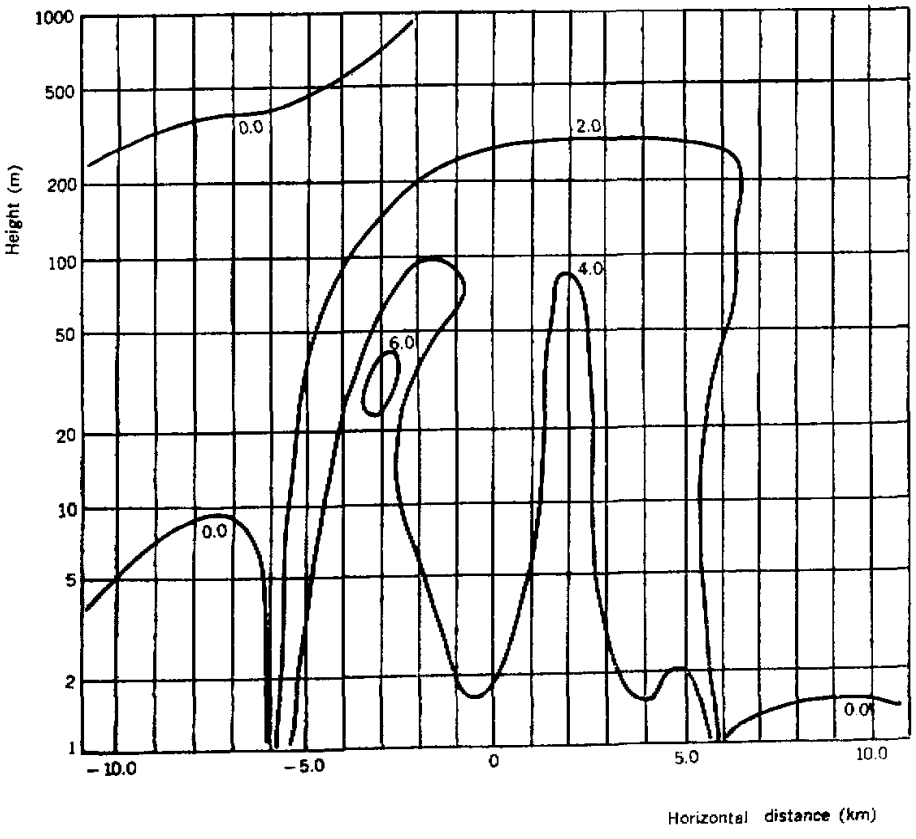

Fig. 1. Vertical section of the disturbance temperature over urban heat island, isolines are °C.

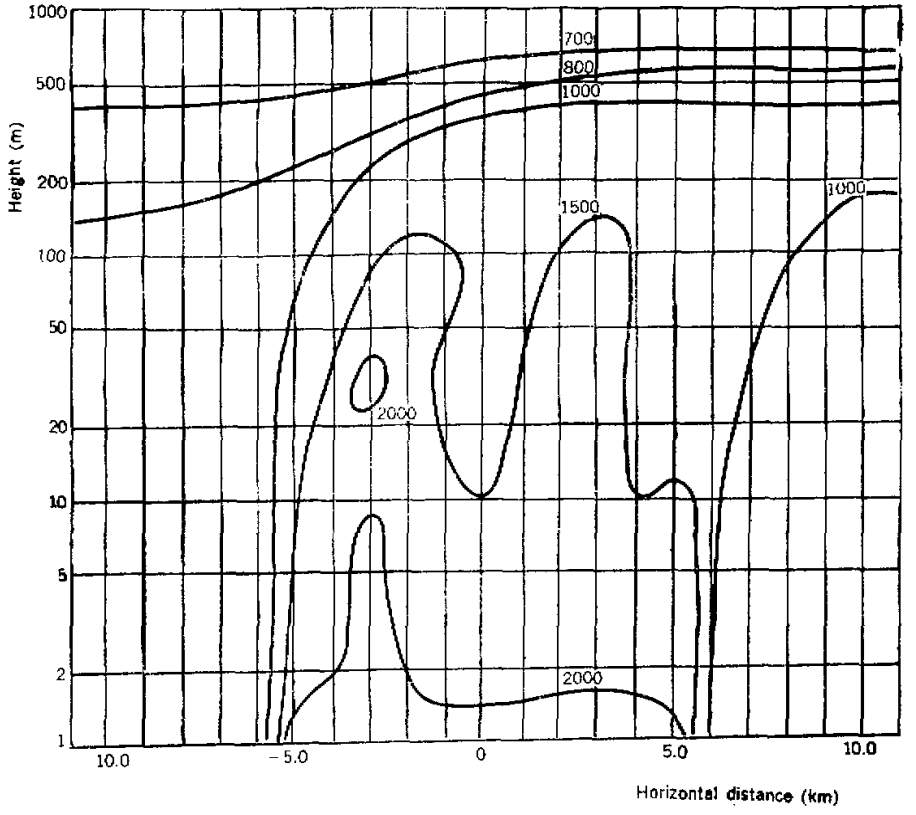

Fig. 2. Vertical section of the dust density over urban heat island, unit $\mu g/m^3$.

The vertical section of the temperature disturbance is shown in Fig. 1. The unit of the isotherm is °C. It may be seen that the 2°C isotherm of the positive temperature disturbance shows the construction of the island shape. The positive temperature disturbance diffuses to the environment all around and to the downstream even more, constructing the thermal plume. In addition, the distribution of the stream field and the eddy coefficient is computed. The vertical section shows that the wind-speed is great in the upstream of the heat island, but it is small in the heat island itself. The downstream of the heat island is a region of the return streamer. A local circulation exists in the downstream of the heat island. The isoline of the eddy coefficient shows that the eddy coefficient in the heat island is greater than that outside, and two maximum centres exist. The maximum is 48.2 m^2/s. The vertical section of the dust density is shown in Fig. 2, the unit is $\mu g/m^3$. Fig. 2 shows the diffusion situation of an area source. It may be seen that a passage transporting the dust to the downstream exists over the downstream of the heat island. The conclusion from the temperature and the density section coincides with Clarke's (1969) observation. Their observation shows that a passage, through which the heat airmass passes out, exists over the downstream of the heat island at night.

2. *The Numerical Modeling for the Construction Characteristics of the Cold Island*

In the summers of 1984 and 1985, we carried out a contrast observation between different underlying surfaces, the Gobi desert being contrasted with farmland and the desert being contrasted with a reservoir. According to the observation, the underlying surface is heterogeneous, so that an oasis or a lake in the desert in comparison with the surrounding environment is a cold source, forming the so-called "cold island effect". The typical temperature profiles are shown in Fig. 3. These profiles were obtained in the desert and Hongyashan Reservoir points in Minqin, Gansu, for 1200–2200 LST on 3rd August 1985. That day was cloudless. The reservoir has a circumference of 4.5 km, and is surrounded by desert.The observational point at the reservoir is situated about 0.7 km from the bank and that at the desert is situated about 1.1 km from the bank. The distance between the two observation points is about 1.8 km. Fig. 3 shows that the air over the desert is in the unstable stratification of the superadiabatic state, but the air over the reservoir is in the stable stratification of the ground inversion. The temperature at the same time on the same level over the desert is higher than that over the reservior: the temperature difference is 5.8 °C at 1 m height at 1400 LST.

For research into the space construction and the physical mechanism of the formation of a cold island, a numerical modeling example of the cold island is given. This time the lower boundary condition of temperature is $\theta=\theta_0-\Delta\theta$ in the cold island, where $\theta_0=300$ K, and $\Delta\theta=5$°C. Here q is the specific humidity. Put $q_0=9$ mg/kg, and $\Delta q=11$ mg/kg. For convenient comparison with the result of the heat island without changing the crux of the matter, the other parameters are the same as in the previous example.

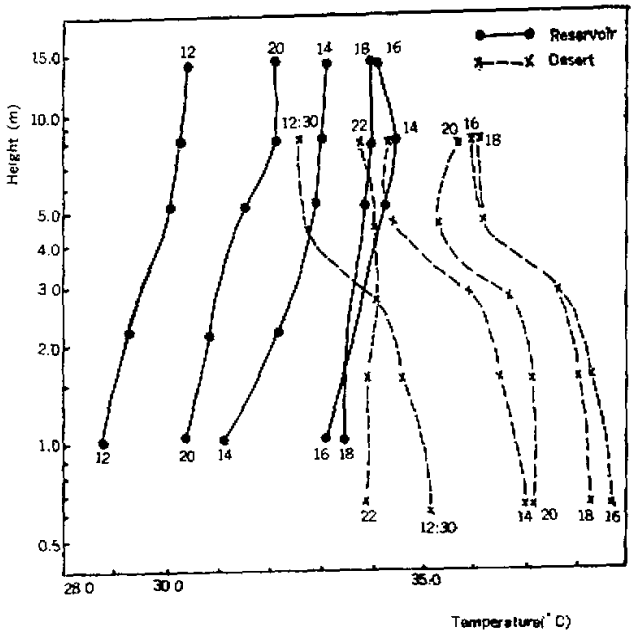

Fig. 3. Temperature profiles over reservoir and desert in period from 1200 to 2200 LST on 3rd August 1985, Abscissa-temperature (°C), ordinate logarithmic height (m). LST indicated on every profile.

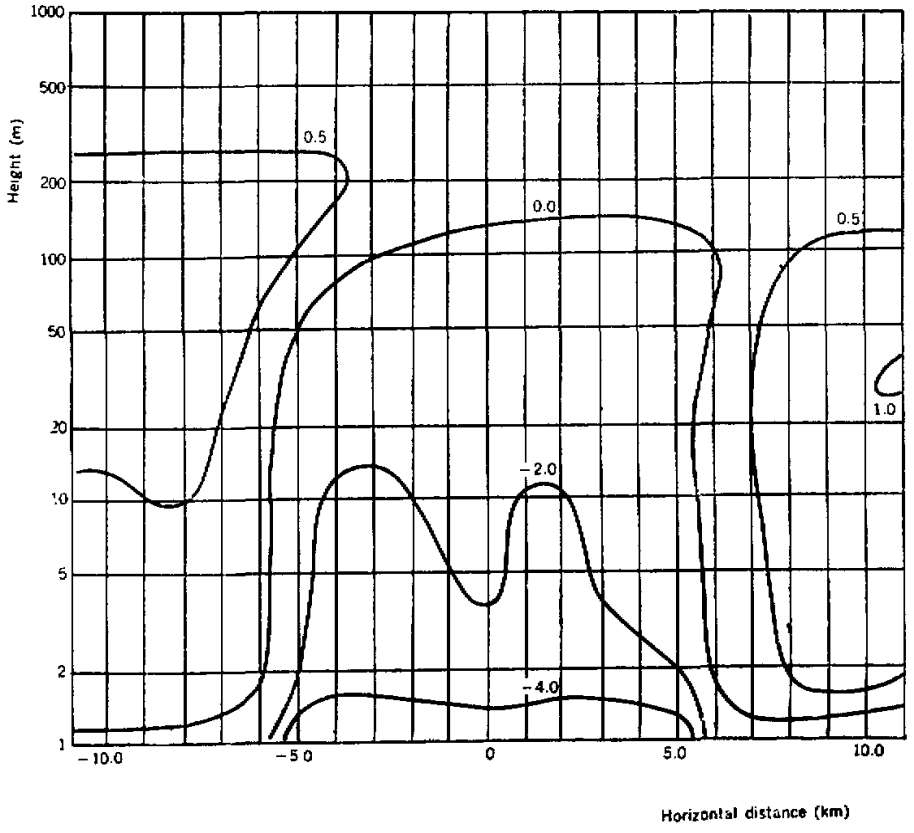

Fig. 4. Vertical section of the disturbance over cold island, unit °C.

Fig. 4 shows the temperature disturbance field. It shows that the 0°C isoline clearly constructs the boundary of the cold island which separates the positive temperature disturbance region from the negative. Due to the advection effect, the heating region over the upstream of the cold island stretches over the cold island. This illustrates that the hot air over the upstream moves over to the cold island.

The vertical temperature profile is given in Fig. 5. It can be seen that the background field is the unstable stratification, but the centre of the cold island is situated in the inversion. It seems that, due to the advection effect the environment heated air moves over to the cold island, causing the above mentioned particular construction which characterizes that the desert is in the superadiabatic unstable stratification, but the reservior is in the strong ground inversion. Fig. 6 shows the specific humidity. The unit is mg/kg. The isohume 10 mg/kg is as the island shape construction as the isothermohyps 0°C in Fig. 4. So it is called the "humid island". It can be concluded from Fig. 4 and Fig. 6 that the cold island and the humid island all stretch to 100 m high. Above 200 m the temperature and the specific humidity tend to uniformize in horizontally. The distribution of computed horizontal wind

velocity shows that the wind-speed is great in the upstream of the cold island, but is small in the downstream. When the air stream passes over the cold island, it encounters a stable cold air parcel and is subjected to resistance, just as when over a little relief. The distribution of the eddy coefficient over the cold island is smaller than that in the upstream and downstream. It is quite natural that this is due to the stable stratification in the cold island.

V. DISCUSSION

(1) By introducing the eddy coefficient of the horizontal heterogeneous shear in stream field and considering the horizontal turbulence exchange in the control equations, numerical model of the planetary boundary layer under horizontal heterogeneity is obtained. The relaxation method is used to obtain the iteration formula of the corresponding difference equation, thus the numerical solution of the control equations can be conveniently found. The numerical tests show that the construction characteristic of some phenomena in the planetary boundary layer is due to the surface heterogeneity.

(2) The numerical model of the cold island explains theoretically some physical mechanisms of its formation. In comparison with the surrounding environment an oasis or lake in the desert is a cold source, which forms the cold island effect, due to the sun heating underlying surface in a different way. Because of advection or local circulation effect, the

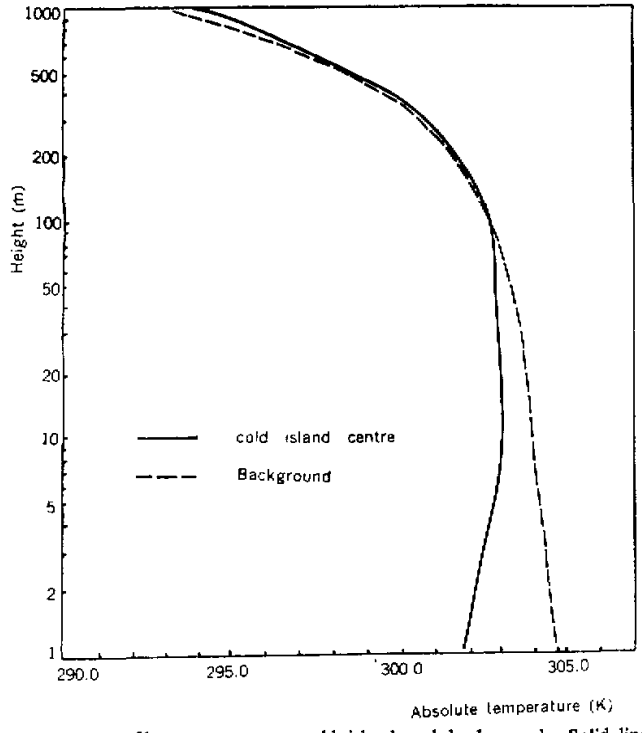

Fig. 5. Temperature profile at centre over cold island and background. Solid line is at centre over cold island and dashed line is background.

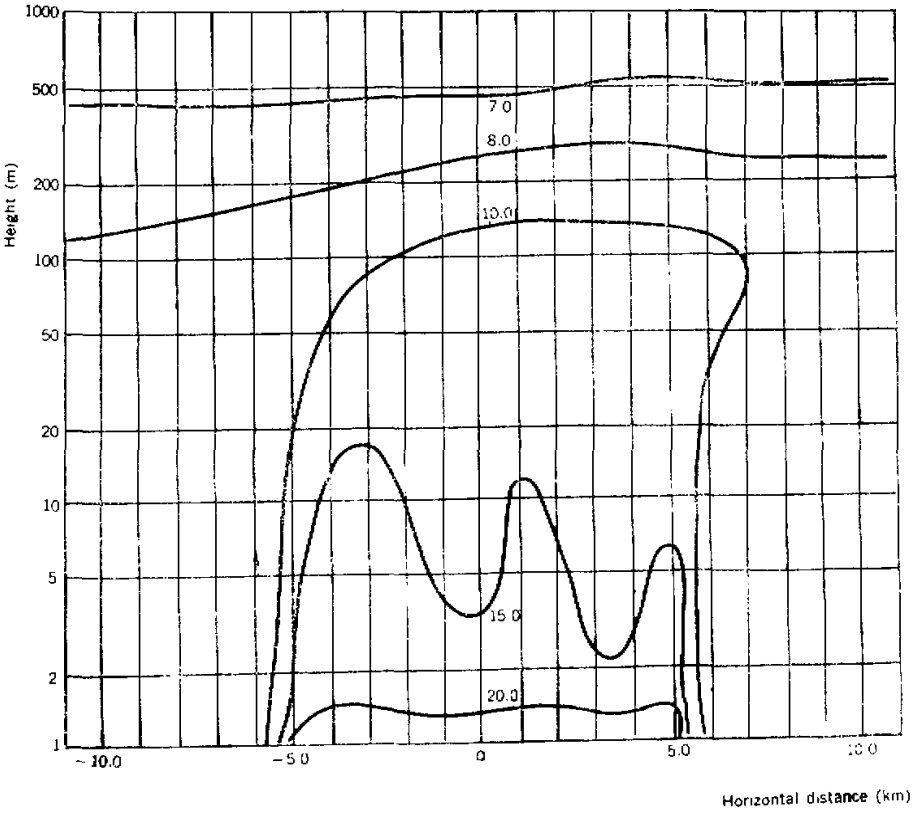

Fig. 6. Vertical section of the specific humidity over cold island, unit mg/kg.

surrounding hot air is transported over to the cold island, the strong ground inversion is formed and maintained for a long time under the sunshine. Thus both turbulence and the evaporation of the oasis or lake are restrained. Our observation of the turbulent flux and evaporation confirms this. The desert is in a condition of drought and intense heat and in the unstability stratification under the summer sunshine, but an oasis and a lake form a stable cool and humid microclimate, which is advantageous to plant growth and natural resources preservation in the Northwest and has economic significance.

(3) Comparing the two examples, it may be seen that although the cold island and the heat island are meteorological phenomena due to the thermal heterogeneity of the underlying surface, their construction has some differences. The cold island is a stable cold-air parcel, having stable stratification inside and a clear boundary, and cannot easily give rise to mass exchange between the inside and outside. A series of phenomena illustrates that the cold island has stable conservation. As opposed to the cold island, the heat island has stratification unstability and an intensive turbulent field and can exchange mass and energy with the outside easily. So its properties diffuse to the surrounding environment and thus the heat island has no clear boundary. It has the diffusion property of intensive turbulence.

(4) This model is essentially a meso-scale model. It is used for the heat and cold island phenomena, which is close to the small-scale problem. Furthermore, this model is two-dimensional but not column coordinate, so the model for the heat island and the cold island phenomena may induce error. Moreover, because of our insufficient knowledge of the horizontal eddy coefficient we should consider how to choose it reasonably. These problems should be improved further, but these problems do not damage the physical character of the subject under research. Therefore this model is useful in researching meteorological phenomena due to underlying surface heterogeneity in the planetary boundary layer.

REFERENCES

Barbato J.P. (1978), Area parameters of the sea breeze and its vertical structure in the Boston Basin, *BAMS.*, **59:** 1420–1431.

Blackadar A.K. (1962), The vertical distribution of wind and turbulent exchange in a neutral atmosphere. *J. Geo. Res.*, **67;** 3095–3102.

Businger J. A. et al. (1971), Flux profile relationships in the atmospheric surface layer, *J. Atmos. Sci.*, **928**:180–190.

Clarke J. F. (1969), Nocturnal urban bounbary layer over Cincinnati Ohio, *Mon. Wea. Rev.*, **97**:582–591.

Estoque M. A. (1962), The sea breeze as a function of the prevailing synoptic situation, *J. Atmos. Sci.*, **19**:244–250.

Heisenberg W. (1948), Zur statistischen Theorie der Turbulenz, *Z. Physik*, **124**:628–657.

Mitchell J., Murray Jr. (1961), The thermal climate of cities, U. S. Public Health Service Report No. Ag 2–5, Cincinnati Ohio, Nov. 1961, PP. 131–145.

Nitta, Ta. (1964), On the reflective computational wave caused by the outflow boundary condition, *J. Met.* (in Japanese), **42**:274–276.

Pielke R.A. (1974), A three dimensional numerical model of the sea breezes over South Florida, *Mon. Wea. Rev.*, **102:** 115–139.

Robert D. Bornshein (1975), The two-dimensional Urbmet urban boundary layer model, *J. App. Met.*, **14:** 1459–1471.